Original Article
Sorting and biological characteristics analysis for side population cells in human primary hepatocellular carcinoma

Yegui Jiang, Hucheng Gao, Mingdong Liu, Qing Mao

Department of Infectious Diseases, Southwest Hospital, Third Military Medical University, Chongqing 400038, China

Abstract: Hepatocellular carcinoma (HCC) is the fifth most common cause of the tumor worldwide, its incidence is increasing year by year. This study aims to investigate the sorting and biological characteristics of side population (SP) cells. Human HCC tissues used were obtained from patients undergoing surgical resection. SP cells were sorted using flow cytometry. Cell cycle assay, apoptosis assay and colony formation assay were performed to detect cell proliferation and apoptosis. Invasion assay was employed to examine SP cell invasion. Tumorigenicity assay was used to evaluate tumorigenicity. HCC related microRNAs (miRNA) were analyzed using Micro-array analysis. Target genes were predicted using miRNA database. GO analsis was employed to predict target gene function. Apoptosis percentage was lower and cell viability was higher in SP cells than non-SP (NSP) cells. Colony forming ability of SP cells was significantly higher than NSP cells. Transwell assay positive cells in SP cells were higher significantly than NSP cells. Tumorigenicity of SP cells was higher significantly than NSP cells. 107 differentially expression miRNA were discovered, including 45 up-expressed miRNAs and 62 down-expressed miRNAs in SP cells. Up-regulated hsa-miR-193b-3p and hsa-miR-505-3p predict 25 and 35 target genes, and correlated with 4 and 42 GO terms, respectively. Down-regulated hsa-miR-200a-3p, hsa-miR-194-5p, hsa-miR-130b-3p predict 133, 48 and 127 target genes, and correlate with 10, 7 and 109 GO terms, respectively. In conclusion, proliferation, colony formation, anti-apoptosis, self-renewal capavility, invasive characteristic and tumorigenicity in SP cells isolated from HCC tissues was higher compared to NSP cells. Therefore, sorted SP cells could characterize with biological functions of cancer stem cells.

Keywords: Hepatocellular carcinoma, side population, biological characteristics, microRNA, cell sorting

Introduction

Hepatocellular carcinoma (HCC) is the fifth most common cause of the tumor worldwide, its incidence is increasing year by year. Meanwhile, the HCC ranks the third deah reason in all of the cancer patients, causing over 500,000 cases deaths annually. China is a higher HCC incidence country in the world [1]. The invasive potential, metastasis, lower surgical resection rate, higher recurrence rate and in-sensitive to chemotherapy are the most important cause for higher mortality of hepatocellular carcinoma. Therefore, the study for the mechanism of HCC development is critical and important for the hepatocellular carcinoma therapy in clinical.

Cancer stem cells (CSC) mainly exist in the tumor cells, which are also a small group of cell-population with the characteristics of stem cells, and could be unlimited self-renewal, promote tumor formation and trigger tumor growth, invasion, metastasis and tumor recurrence [2-4]. The researchers firstly found a small amounts of leukemia stem cells in the leukemia cells, and which characterizes with CSC features [5-10]. However, due to lack of specific surface markers for hepatocellular carcinoma, there are also seldom studies for the hepatocellular carcinoma stem cells [11, 12].

Since there is ATP binding cassette transporter protein superfamily G2 (ABCG2) on the surface of a great majority of stem cells, which could transport the exogenous DNA fluorescent dye, Hoeschst33342, to the outside of cells, therefore the stem cells can't be stained. This kind of cells, which can't stained by the Hoeschst333-

42, are called side population (SP) cells. Goodell et al. [13] firstly isolated a small-population of SP cells from the mice marrow. The isolated SP cells could express the surface markers of hematopoietic stem cells, and even one in a thousand amouts of SP cells could re-construct the bone marrow hematopoietic system. Subsequently, the SP cells wwere also isolated from a series of mormal tissues [14-19], tumor tissues and the tumor cell lines [20-34]. This conservative phenotype of SP cells demonstrate that the distinct tissue-derived stem cells possess some of the common characteristics.

The current studies mainly discuss the hepatocellular carcinoma SP cells in the hepatocellular carcinoma cell lines [35-40], and seldom studies isolating SP cells from human hepatocellular carcinoma tissues were reported [41]. This study sorted and selected the SP cells from human hepatocellular tissues by using the fluorescence-activated cell sorting technique taking advantage of efflux characteristics of Hoechst33342. Meanwhile, we also analyzed the relevant biological characteristics of SP cells, investigated the existance of tumor stem cell-featured SP cells in human hepatocellular carcinoma. This study would lay the foundations for the screening and sorting the hepatocellular carcinoma stem cells, and for the targeting therapy for the hepatocellular carcinoma.

Materials and methods

Clinical samples and cell culture

Human hepatocellular carcinoma tissues used in this study were obtained from patients undergoing surgical resection after informed consent. All these patients (10 in total, 8 males, 2 females, age from 32 to 76) were admitted into Southwest Hospital between January, 2011 and December, 2012, and were diagnosed with primary hepatocellular carcinoma and received no previous chemotherapy or radiation therapy. Briefly, fresh tumor samples obtained within 60 min of surgery were rinsed, mechanically minced, and digested for 30 minutes at 37°C shaking incubator with 0.1% collagenase VI (Sigma, CA, USA), 100 U/ml penicillin (Sigma) and 100 mg/ml streptomycin (Sigma) in DMEM (Gibico, CA, USA). The digest was further disaggregated through an 100 μm

cell strainer (Millipore, MI, USA) to obtain the single cell suspension. The single cell suspension was then centrifuged for 5 min at 1000 r/min twice and 4 min at 800 r/min twice after discarding the supernatant each time. The cell sediment was suspended in DMEM with 10% fetal bovine serum (FBS, Gibico) and incubated in a humidified incubator at 37°C supplied with 5% carbon dioxide at a concentration of $1×10^9$/L per flask. After 24 h of incubation, the media needed to be changed to 10 μg/ml insulin (Sigma), 1 mmol/L L-glutamine (Sigma), 1% penicillin and streptomycin (Sigma) and 10% FBS in DMEM. Afterwards, cells were harvested and replanted every three days.

SP cell sorting

The cell suspensions were labeled with Hoechst 33342 dye (Sigma) using the methods described by Goodell et al. [7], and with a few modifications. Briefly, cells were resuspended at $1×10^6$/mL in prewarmed DMEM (Gibico) with 10% FBS (Gibico) and 10 mmol/L HEPES buffer (Bioshop, CA, USA). Hoechst 33342 dye was added to a final concentration of 5 μg/mL in the presence or absence of verapamil (50 μg/L; Merk, Germany). Then, the cells were incubated at 37°C for 90 min with intermittent shaking. At the end of the incubation, cells were washed with ice-cold HBSS (Invitrogen-Life Technologies) with 2% FBS and 10 mmol/L HEPES, centrifuged down at 4°C, and resuspended in ice-cold HBSS containing 2% FBS and 10 mmol/L HEPES. Propidium iodide (PI; Sigma) at a final concentration of 2 μg/mL. Then the cells were filtered through a 40 μm cell strainer (Millipore) to obtain single cell suspension before sorting. Analyses and sorting were done on a FACSVantage SE (MoFlo™ XDP Flow Cytometer, BECKMAN COULTER, Germany). The Hoechst 33342 dye was excited at 357 nm and its fluorescence was dual-wavelength analyzed (blue, 447/60 nm; red, 615/20 nm).

Real-time quantitative PCR

Total RNA was extracted by using TRIzol reagent (Invitrogen, CA, USA), followed by first strand cDNA syhthesis using SuperScript™ III reverse transcriptase (Invitrogen, CA, USA) for RT-PCR as directed by the manufacturer's protocol. Real-time PCR was carried out using SYBR-Green Real-Time Core Reagents (Applied Biosystems) on an ABI Prism 7900 Sequence

Detection System (Applied Biosystems, Foster City, CA). The primers for PCR were listed as the follows: ABCG2, 5'-GATAAAGTGGCAGACTCCA-AGGT-3', and 5'-CCAATAAGGTGAGGCTATCAA ACA-3'; GAPDH, 5'-GGGAAACTGTGGCGTGAT3', and 5'-GAGTGGGTGTCGCTGTTGA-3'. The PCR cycle conditions were 95°C for 10 min, followed by 40 cycles of 95°C for 10 sec and 60°C for 60 sec. All reactions were performed in triplicate for each sample primer set, and the experiment was repeated three times. ΔCt (cycle threshold) was calculated for each sample (ΔCt = Ct_{ABCG2}-Ct_{GAPDH}), and relative quantities were compared.

Cell cycle assay

For the cell cycle assay, freshly sorted SP and non-SP cells were washed twice with PBS and then 0.5 ml cell suspension was slowly added into 75% ice-cold ethanol at 4°C overnight. Cells were then washed 3 times by PBS, stained with PBS plus 5 µg/ml PI and 200 µg/ml RNase A and 0.1% Triton X-100. Then the cells were analyzed using flow cytometry. The results were expressed as the percentage of cells in each phase of the cell cycle. Proliferation index (PI) was calculated via PI = 100 (S+G2/M)/(G0/G1+S+G2/M).

Apoptosis assay

Sorted SP or non-SP cells were treated with 0.25% trypsin and washed twice with PBS. The cells were then stained with Annexin-V and PI using the Vybrant Apoptosis Assay Kit (Molecular Probes) as per the manufacturer's protocol. Briefly, the cell pellets were resuspended in 100 µl 1× Annexin binding buffer and 5 µl fluorescein isothiocyanate (FITC)-Annexin-V (component A). A 1-µl working solution of PI at 100 µg/ml was added to each 100 µl of cell suspension. The cells were incubated on ice for 1 h, washed again with cold PBS and resuspended in 300 µl 1× Annexin-binding buffer. The stained cells were immediately analyzed by flow cytometry.

Fresh sorted SP and MP cells were seeded immediately at 1×10³ cells per well in 96-well plates and incubated in a humidified incubator at 37°C supplied by 5% carbon dioxide. 20 µl 3-[4,5-dimethylthiazol-2-yl]-2,5-diphenyltetra-zolium bromide (MTT) was added to each well after 24-hour incubation. After another 4 hour incubation, culture medium was removed before 150 µl DMSO was added. The plate was

then shaked mildly for 10 min in room temperature before it was ready to measure the absorbance. We read the absorbance at the wavelength of 490 nm from a Bio-Rad enzyme reader every 24 hour for 8 days consecutively and plotted the growth curve accordingly.

The procedure was repeated three times.

Colony formation assay

Newly sorted SP and NSP (non-SP) cells were seeded into 6-well plate respectively at 1000 cells per well and then incubated in a humidified incubator at 37°C supplied with 5% carbon dioxide for 14 days until visible colonies grew out. When most cell clones reached more than 50 cells, they were washed twice with PBS, fixed in methanol for 15 min, and stained with crystal violet dye for 15 min at room temperature. Colonies with more than 50 cells or a diameter larger than 75 µm was counted. The colony formation efficiency (CFE) was calculated via CFE = colony number/seeded cell number.

Invasion assay

Cellular potential for invasiveness of SP and non-SP cells was determined using six-well Matrigel invasion chambers (BD Biosciences Discovery Labware). Cells were seeded into upper inserts at 5×10⁵ per insert in serum-free DMEM. Outer wells were filled with DMEM containing 10% FBS as chemoattractant. Cells were incubated at 37°C with 5% carbon dioxide for 48 h, and then noninvading cells were removed by swabbing top layer of Matrigel with Q-tip. Membrane containing invading cells was first fixed with 95% ethanol for 15 min and then stained with hematoxylin for 15 min, washed, and mounted on slides. The entire membrane with invading cells was counted under light microscope at 200 objective.

Tumorigenicity assay in vivo

Athymic 4- to 5-week-old mice (BALB/c nude mice) were supplied by the Animal Research Center of Third Military Medical University, Chongqing, China. Mice were housed and maintained in laminar flow cabinets under pathogen-free conditions, and the experiments performed in accordance with regulations and standards for experimental animals of China. Freshly sorted SP and non-SP cells were resuspended in PBS at concentrations of 10³, 10⁴

and 10^5 per 50 μl. Groups of mice were ortho-topically inoculated with varying numbers of SP and non-SP cells (three mice per group). Tumor growth was monitored every three days. The mice were sacrificed at day 32. The tumor was then taken out and fixed with 10% methhy-drate. Then the tumor tissue was prepared for slicing and HE staining.

Micro-array analysis

Total RNA was isolated using TRIzol (Invitrogen, CA, USA) and miRNeasy mini kit (QIAGEN, Beijing, China) according to manufacturer's instructions, which efficiently recovered all RNA species, including miRNAs. After having passed RNA quantity measurement using the NanoDrop 1000 (Nanodrop Technologies, USA), the sam-ples were labeled using the miRCURY™ Hy3™/ Hy5™ Power labeling kit (Exiqon, Vedbaek, Denmark) and hybridized on the miRCURY™ LNA Array version 18.0 (Exiqon, Vedbaek, Denmark) according to manufacturer's instruc-tions. This array contains 3100 capture probes, covering all human, mouse and rat microRNAs annotated in miRBase 18.0, as well as all viral microRNAs related to these species. In addi-tion, this array contains capture probes for 25 miRPlus™ human microRNAs, which are propri-etary microRNAs not found in miRBase. Following the washing steps the slides were scanned using the Axon GenePix 4000B micro-array scanner (Axon Instruments, Foster City, CA). Scanned images were then imported into GenePix Pro 6.0 software (Axon Instruments, Foster City, CA) for grid alignment and data extraction. Replicated miRNAs were averaged and miRNAs that intensities ≥30 in all samples were chosen for calculating normalization fac-tor. Expressed miRNA data were normalized using the Median normalization and chosen for differentially expressed miRNAs screening. To identify differentially expressed miRNAs, we performed a Fold Change filtering between the two samples from the experiment. The thresh-old we used to screen Up or Down regulated miRNAs is Fold Change ≥2.0.

Identification for microarray results

In order to indetiry the accuracy of the microar-ray results, the 12 differentially expression miRNAs in the above 3 cases were seleted in this study (including 2 men, 1 woman. The age is 37, 47 and 51 years, respectively). The iso-lated SP and NSP were detected by using the RT-PCR assay. The specific method was per-formed due to the above method ("miRNA micro-array assay" section), and the U6 was assigned as the internal control. The RT-PCR assay condictions were listed as the followings: 95°C, 10 min, and 95°C for 10 sec and 60°C for 60 sec (for 40 cycles). The primers were listed in **Table 1**.

Target gene prediction and function analysis

Five differentially expressed miRNAs (2 up-reg-ulated miRNAs, including hsa-miR-193b-3p and hsa-miR-505-3p. Three down-regulated miRNAs, including hsa-miR-200a-3p, hsa-miR-194-5p and hsa-miR-130b-3p) were seleted for the target gene prediction by using the mir-base (http://www.ebi.ac.uk/enright-srv/micro-cosm/htdocs/targets/v5), miranda (http://www.microrna.org/microrna/home.do) and tar-getscan (http://www.targetscan.org/vert_60/) databases. The Gomir analysis software was also used to screen the overlapping genes among the above 3 databases. GO analis was employed to predict the function of the target genes.

GO analysis

The Gene Ontology project provides a con-trolled vocabulary to describe gene and gene product attributes in any organism (http://www.geneontology.org). The ontology covers three domains: Biological Process, Cellular Com-ponent and Molecular Function. Fisher's exact test is used to find if there is more overlap between the DE list and the GO annotation list than would be expected by chance. The *P*-value denotes the significance of GO terms enrich-ment in the DE genes. The lower the *P*-value, the more significant the GO Term (*P*-value ≤0.05 is recommended).

Statistical analysis

All of the data were reported as mean ± SD, and analyzed by using the SPSS (version 11.0). The Student's t test and χ^2 test were used to identify the statistically significant difference bet-ween or among groups. A *P* value less than 0.05 was considered as statistically significant.

Results

SP cell sorting via flow cytometry

In this study we used the Hoechst33342 meth-od to analyze the SP cell sorting by using the

Table 1. Primers used to perform RT-PCR of miRNAs

miRNA name	RT primers (5'→3')	PCR primers (5'→3')
hsa-miR-193b-3p	5'-GTCGTATCCAGTGCGTGTCGTGGAGTCGGCAATTGCACTGGATACGACAGCGGGA-3'	GSP: 5'-GGGAACTGGCCCTCAAAG-3' R: 5'-GTGCGTGTCGTGGAGTCG-3'
hsa-miR-16-2-3p	5'-GTCGTATCCAGTGCGTGTCGTGGAGTCGGCAATTGCACTGGATACGACTAAAGC-3'	GSP: 5'-GGGGACCCAATATTACTGTGCT-3' R: 5'-GTGCGTGTCGTGGAGTCG-3'
hsa-miR-4534	5'-GTCGTATCCAGTGCGTGTCGTGGAGTCGGCAATTGCACTGGATACGACAGACCC-3'	GSP: 5'-GGGAAGGGATGGAGGAGG-3' R: 5'-GTGCGTGTCGTGGAGTCG-3'
hsa-miR-505-3p	5'-GTCGTATCCAGTGCGTGTCGTGGAGTCGGCAATTGCACTGGATACGACAGGAAA-3'	GSP: 5'-GGCGTCAACACTTGCTGG-3' R: 5'-GTGCGTGTCGTGGAGTCG-3'
hsa-miR-4441	5'-GTCGTATCCAGTGCGTGTCGTGGAGTCGGCAATTGCACTGGATACGACTACAAT-3'	GSP: 5'-GGGGGATACAGGGAGGAGA-3' R: 5'-GTGCGTGTCGTGGAGTCG-3'
hsa-miR-5187-3p	5'-GTCGTATCCAGTGCGTGTCGTGGAGTCGGCAATTGCACTGGATACGACCTGAGG-3'	GSP: 5'-GGGGGGACTGAATCCTCTTT-3' R: 5'-GTGCGTGTCGTGGAGTCG-3'
hsa-miR-200a-3p	5'-GTCGTATCCAGTGCGTGTCGTGGAGTCGGCAATTGCACTGGATACGACACATCG-3'	GSP: 5'-GGGGGTAACACTGTCTGGTAA-3' R: 5'-GTGCGTGTCGTGGAGTCG-3'
hsa-miR-194-5p	5'-GTCGTATCCAGTGCGTGTCGTGGAGTCGGCAATTGCACTGGATACGACTCCACAT-3'	GSP: 5'-GGGGGTGTAACAGCAACTCC-3' R: 5'-GTGCGTGTCGTGGAGTCG-3'
hsa-miR-130b-3p	5'-GTCGTATCCAGTGCGTGTCGTGGAGTCGGCAATTGCACTGGATACGACATGCCC-3'	GSP: 5'-GGGGGTGCAATGATGAAA-3' R: 5'-GTGCGTGTCGTGGAGTCG-3'
hsa-miR-125a-3p	5'-GTCGTATCCAGTGCGTGTCGTGGAGTCGGCAATTGCACTGGATACGACGGCTCC-3'	GSP: 5'-GGGGACAGGTGAGGTTCTTG-3' R: 5'-GTGCGTGTCGTGGAGTCG-3'
hsa-miR-3168	5'-GTCGTATCCAGTGCGTGTCGTGGAGTCGGCAATTGCACTGGATACGACGTCTGA-3'	GSP: 5'-GGGGGGGGGAGTTCTACAGT-3' R: 5'-GTGCGTGTCGTGGAGTCG-3'
hsa-miR-361-5p	5'-GTCGTATCCAGTGCGTGTCGTGGAGTCGGCAATTGCACTGGATACGACGTACCC-3'	GSP: 5'-GGGGGTTATCAGAATCTCCAG-3' R: 5'-GTGCGTGTCGTGGAGTCG-3'
U6	5'-CGCTTCACGAATTTGCGTGTCAT-3'	F: 5'-GCTTCGGCAGCACATATACTAAAAT-3' R: 5'-CGCTTCACGAATTTGCGTGTCAT-3'

Note: GSP is the specific primers. F: forward primer; R: reverse primer.

flow cytometry. In order to identify the SP cell in the sorted hepatoma carcinoma cell, the verapamil was used to block the Hoechst33342 staining. When the amounts of the SP cell subpopulation after verapamil treatment was decreased to less then 0.1% or 0, the SP cells were confirmed existing in the hepatoma carcinoma cells. The results indicated that the SP cell percentage was decreased signifcantly in Hoechst33342 + verapamil cells (0.651%) compared to the Hoechst33342 cells (0.026%) (**Figure 1A**, P<0.001).

In order to confirm the SP sorting results of **Figure 1A**, the ATP-binding cassette superfamily G member 2 (ABCG2) was examined in this study. The results indicated that the ABCG2 mRNA levels in Hoechst33342 + verapamil cells were significantly decreased compared to the Hoechst33342 cells (**Figure 1B**, P<0.001).

Cell cycle, cell apoptosis and cell proliferation evaluation

The cell cycle results showed that the percentage of G1 phase in SP cells were significantly higher compared to the NSP cells (**Figure 2A**, P<0.01), and the percentage of S phase in SP cells were significantly lower compared to the NSP cells (**Figure 2A**, P<0.01). Moreover, there were no differences for the G2 stage cells between the SP cells and NSP cells (**Figure 2A**, P>0.05).

The cell apoptosis was also eamined by using the cytometry assay. The results indicated that the cell percentage in SP cells (18.5%) were significantly lower compared to the NSP cells (58%) (**Figure 2B**, P<0.01). Meanwhile, the cell viability was also observed by employing the MTT assay. The MTT results indicated that the there were not significant differences for cell viabiltiy between the SP cells and NSP cells from day 1 to day 3 (**Figure 2C**, P>0.05). However, the cell viability was significantly increased in SP cells compared to the NSP cells from day 4 to day 7 (**Figure 2C**, P<0.05).

Colony formation assay

In order to observe the colony formation in both of the SP cells and NSP cells, the plate colony formation assay and agar colony formation
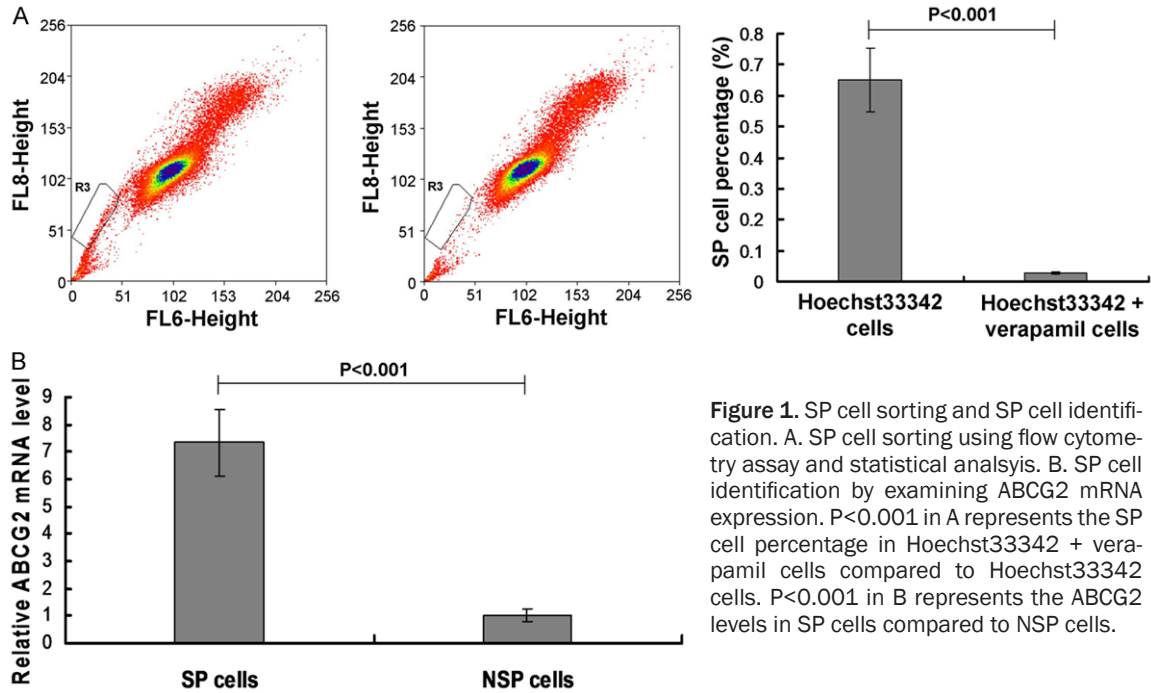
Figure 1. SP cell sorting and SP cell identification. A. SP cell sorting using flow cytometry assay and statistical analsyis. B. SP cell identification by examining ABCG2 mRNA expression. P<0.001 in A represents the SP cell percentage in Hoechst33342 + verapamil cells compared to Hoechst33342 cells. P<0.001 in B represents the ABCG2 levels in SP cells compared to NSP cells.
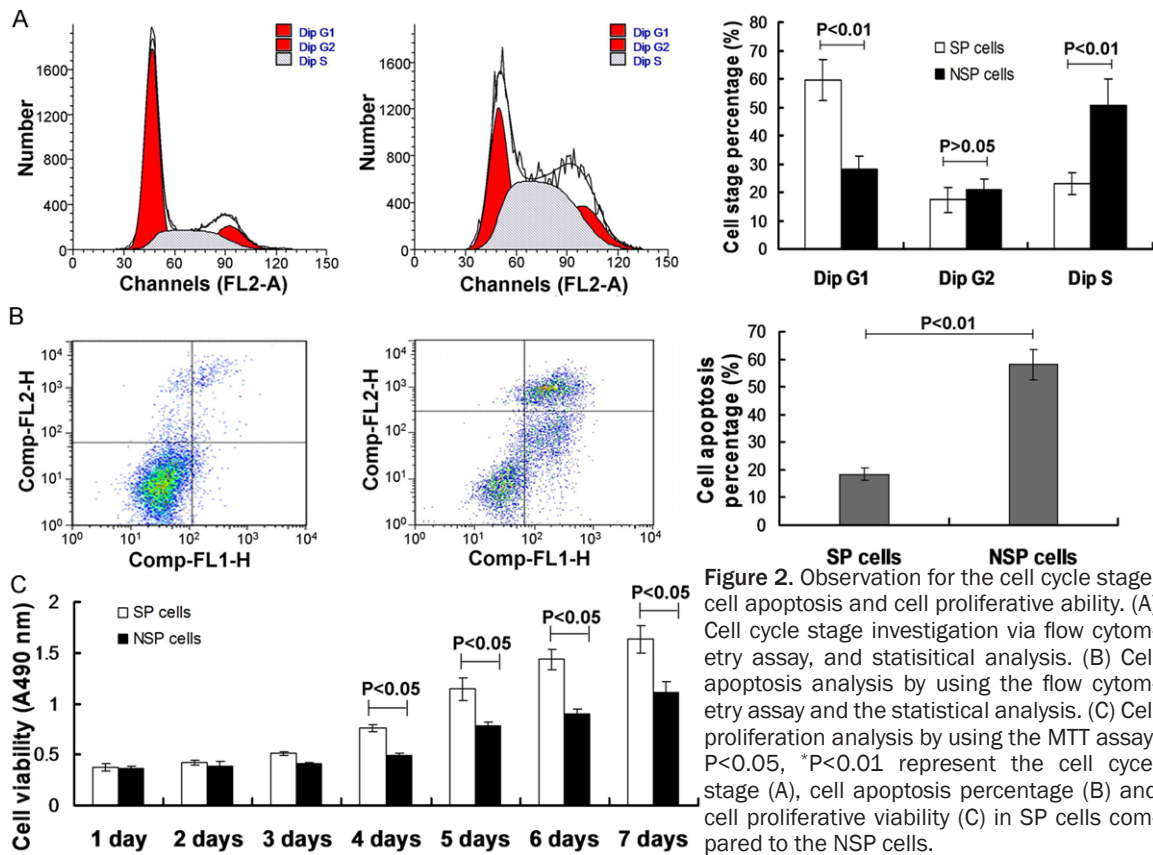

Figure 2. Observation for the cell cycle stage, cell apoptosis and cell proliferative ability. (A) Cell cycle stage investigation via flow cytometry assay, and statisitical analysis. (B) Cell apoptosis analysis by using the flow cytometry assay and the statistical analysis. (C) Cell proliferation analysis by using the MTT assay. P<0.05, *P<0.01 represent the cell cycel stage (A), cell apoptosis percentage (B) and cell proliferative viability (C) in SP cells compared to the NSP cells.

assay were performed in this study. The plate colony formation assay results indicated that there were colony formation both in SP cells and NSP cells under the microscopy. The colony forming efficiency (CFE) in SP cells (27.83%) was significantly higher compared to the NSP
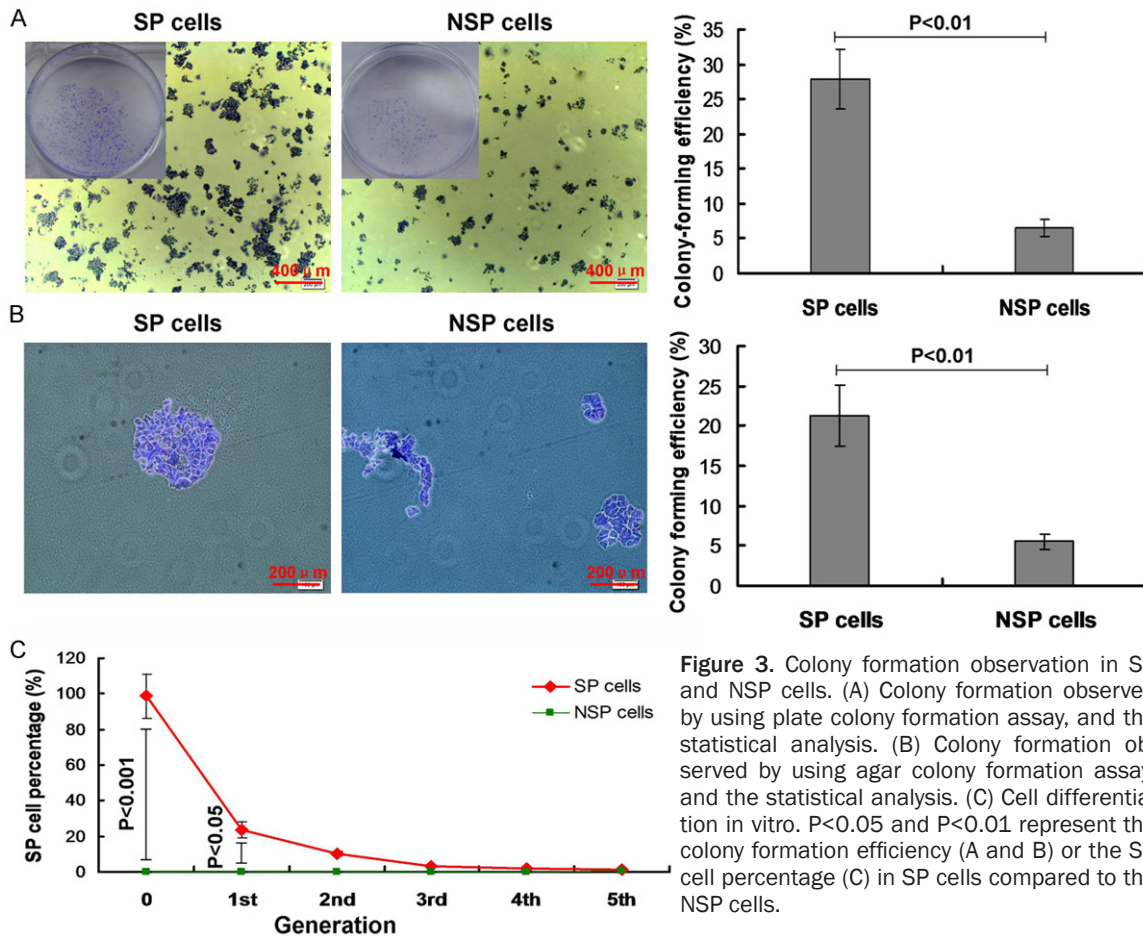
Figure 3. Colony formation observation in SP and NSP cells. (A) Colony formation observed by using plate colony formation assay, and the statistical analysis. (B) Colony formation observed by using agar colony formation assay, and the statistical analysis. (C) Cell differentiation in vitro. P<0.05 and P<0.01 represent the colony formation efficiency (A and B) or the SP cell percentage (C) in SP cells compared to the NSP cells.
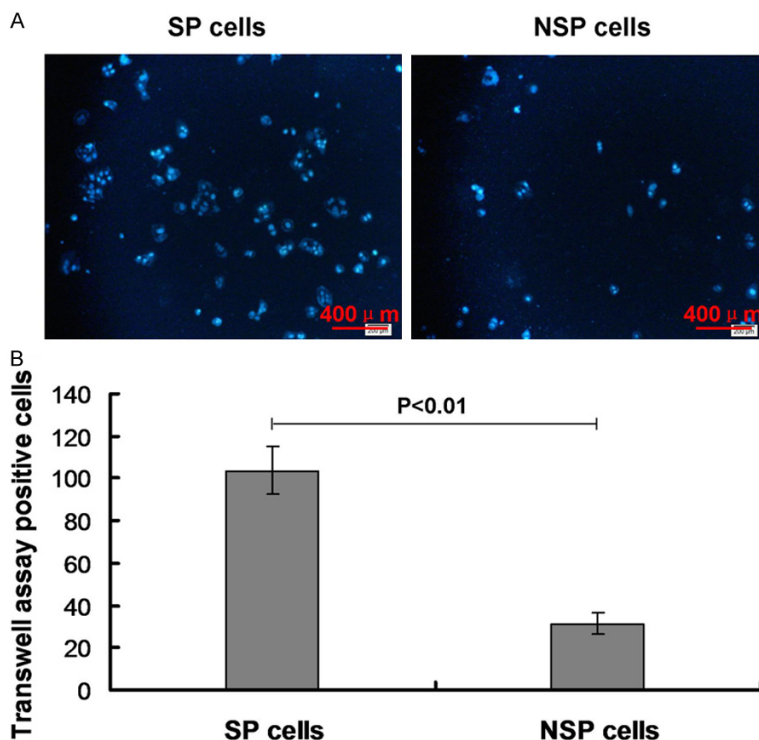

Figure 4. Transwell assay for investigating the invasive capability of SP cells. A. Transwell assay in both SP and NSP cells. B. Statistical analysis for the Transwell assay in vitro. P<0.01 represents the transwell positive cells in SP cells compared to the NSP cells.

cells (6.5%) (**Figure 3A**, P< 0.01). The agar formatin assay results indicated that the diameter of colony in SP cells was longher, and the diameter in NSP cells was shorter. Similar to the plate colony formation resuts, the CFE in SP cells (21.27%) was significantly higher compared to the NSP cells (5.5%) (**Figure 3B**, P< 0.01) in the agar colony formation assay. Both of plate and agar formation assay results suggest that the colo-
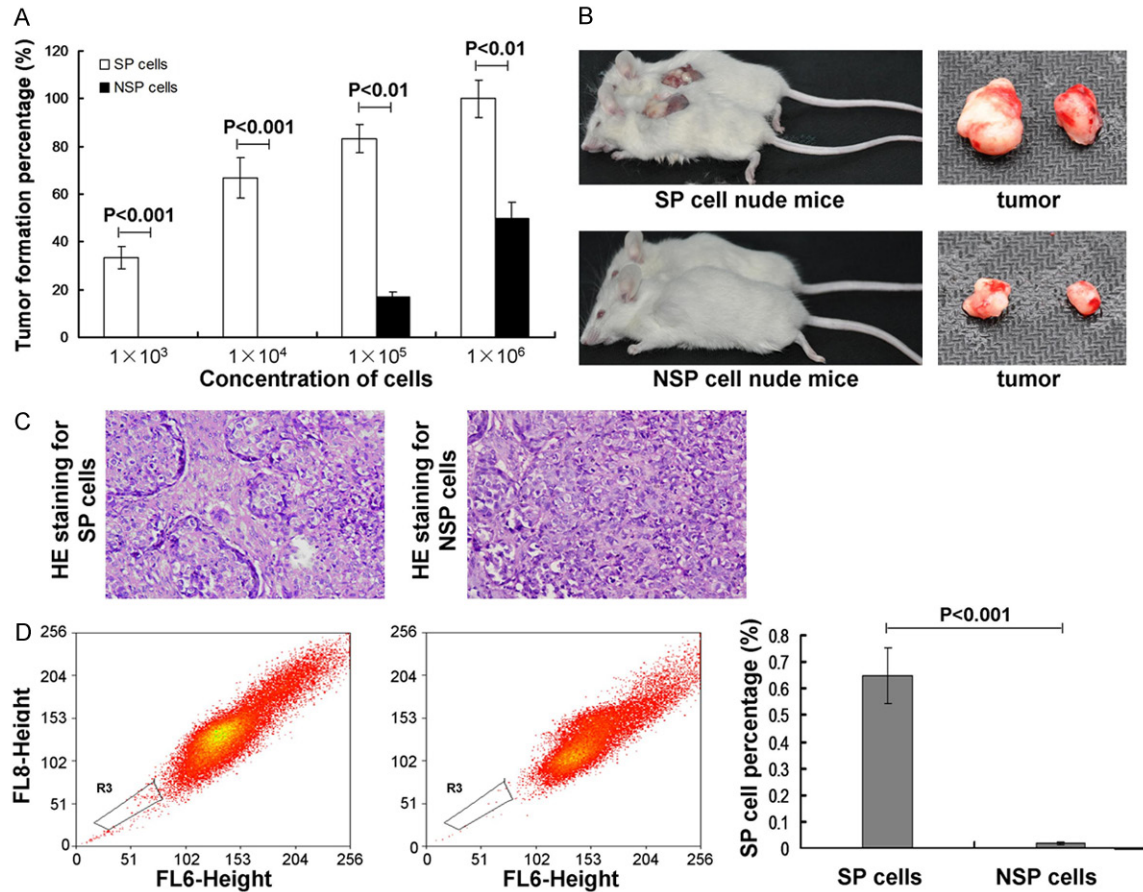
Figure 5. Observation for the tumor formation by using tumorigenicity assay. A. Transplantation tumor formation at different concentrations of cells at the 8 weeks in both SP cells and NSP cells. B. The SP cell or NSP cells nude mice and the transplantation tumors. C. HE stiaining for the histo-morphology for SP or NSP originated tumor tissues. D. SP cell percentage in the transplanted tumors. $P<0.01$ represents the tumor formation percentage in SP cell nude mice compared to NSP cell nude mice. $P<0.001$ represents the SP cell percentage in SP cell nude mice compared to NSP cell nude mice.

ny forming ability of SP cells was significantly higher compared to NSP cells.

Cell differentiation in vitro

According to the results of **Figure 3A**, **3B**, we found that the colony formaion ability was higher in SP cells. Therefore, we also analyzed the cell differentiation in vitro. The results indicated that there was higher SP cell percentage in SP cell group at the first generation and the second generation compared to the NSP cells (**Figure 3C**, $P<0.001$ and $P<0.05$, respectively). Moreover, there were even no NSP cells differentiated into SP cells at every generation.

Transwell assay

To investigate the cell invasive capability of the SP cells, the Transwell assay was performed.

The results indicated that the Transwell assay positive cells (103.8%) in SP cells were higher significantly compared to NSP cells (31.4%) (**Figure 4**, $P<0.01$). This result suggests that the invasive capability of SP cells was higher than then NSP cells.

Tumorigenicity assay in vivo

The tumorigenicity assay results indicated that the SP cells could form the obvious subcutaneous transplantation tumor at the 8 weeks at the concentration of 1×10^3, however, the NSP cells must achieve to the concentration of 1×10^5. The tumor formation percentage in SP cells were significantly higher compared to the NSP cells at every concentratons, including, 1×10^3, 1×10^4, 1×10^5 and 1×10^6, respectively (**Figure 5A**, all $P<0.01$). Meanwhile, the tumor size in
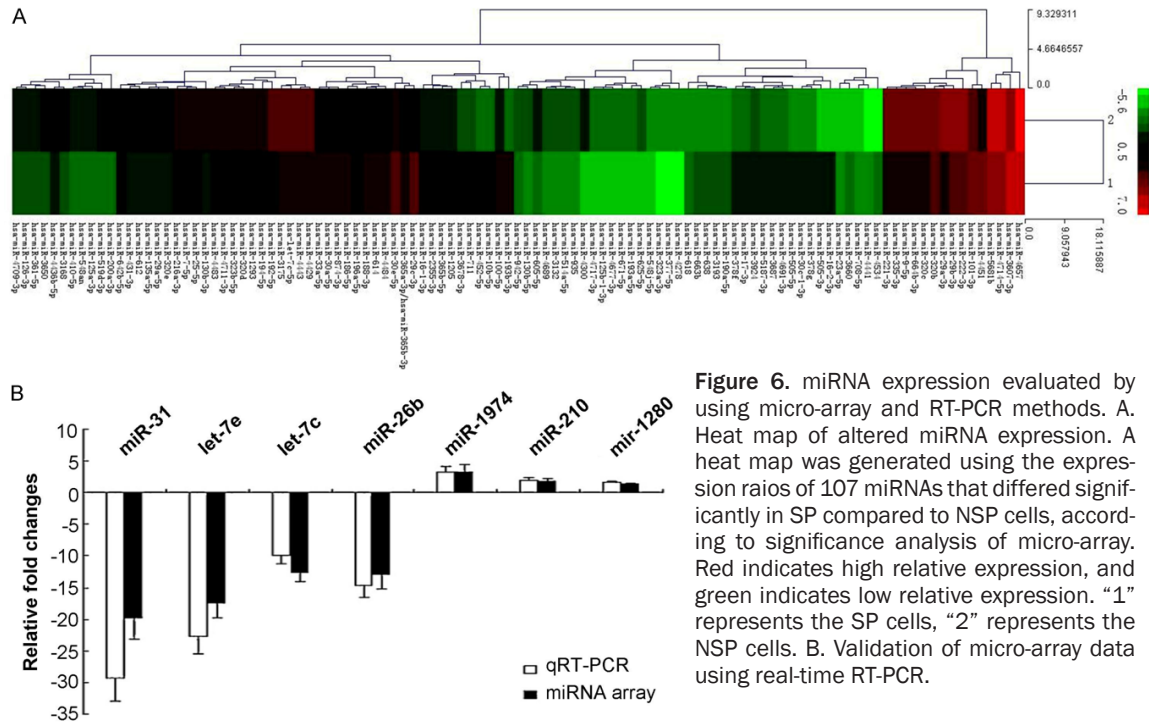
Figure 6. miRNA expression evaluated by using micro-array and RT-PCR methods. A. Heat map of altered miRNA expression. A heat map was generated using the expression raios of 107 miRNAs that differed significantly in SP compared to NSP cells, according to significance analysis of micro-array. Red indicates high relative expression, and green indicates low relative expression. "1" represents the SP cells, "2" represents the NSP cells. B. Validation of micro-array data using real-time RT-PCR.

SP cell nude mice was also biggher obviously compared to the NSP cell nude mice (**Figure 5B**). These resutls recommend that tumorigenicity of SP cells was higher significantly compared to the NSP cells.

In order to evaluate the characteristics of the transplantated tumor, the HE staining and flow cytometry assay were performed. The HE stianing results showed that histo-morphology of the SP cell originated tumor tissues are same to the metrocyte originated tumor tissues, howeve, it is different for the NSP cell originated compared to metrocyte originated tumor tissues (**Figure 5C**). The flow cytometry results indicated that the SP cell percentage in the transplanted tumor was decreased signifcantly in Hoechst33342 + verapamil cells (0.65%) compared to the Hoechst33342 cells (0.02%) (**Figure 5D**, P<0.001). Both of the HE stianing and flow cytometry results suggest that the transplantated tumor tissues retain the characteristics of the SP metrocyte.

Chip results identified by miRNA micro-array analyasis and RT-PCR assay

The miRNA micro-array results indicated that there were 107 differentially expressed miRNA in SP and NSP cells. Among these 107 differentially expression miRNA, 45 miRNAs were up-expressed and 62 miRNAs were down-expre-

ssed in SP cells (**Figure 6A**; Supplementary Table 1).

The up-expressed miRNAs (hsa-miR-193b-3p, hsa-miR-16-2-3p, hsa-miR-4534, hsa-miR-505-3p, hsa-miR-4441, hsa-miR-5187-3p) and the down-expressed miRNAs (hsa-miR-200a-3p, hsa-miR-194-5p, hsa-miR-130b-3p, hsa-miR-125a-3p, hsa-miR-3168, hsa-miR-361-5p) were selected to performed the RT-PCR assay to identify the micro-array results. The RT-PCR results were equal to the miRNA micro-array detection results, and without differences (**Figure 6B**, P>0.05).

miRNA target gene prediction and functional analysis

We seleted two up-regulated miRNAs, including hsa-miR-193b-3p and hsa-miR-505-3p, to predict the target genes. The results indicated that the hsa-miR-193b-3p predicts 25 target genes, and hsa-miR-505-3p predicts 35 target genes (**Figure 7A**, **7B**). The three down-regulated miRNAs, including, hsa-miR-200a-3p, hsa-miR-194-5p, hsa-miR-130b-3p, have also been used to predict the target genes. The results showed that hsa-miR-200a-3p predicts 133 target genes (**Figure 7C**), hsa-miR-194-5p predicts 48 target genes (**Figure 7D**) and hsa-miR-130b-3p predicts 127 target genes (**Figure 7E**).

Figure 7. Graph for the hsa-miR-193b-3p, hsa-miR-505-3p, hsa-miR-200a-3p, hsa-miR-194-5p and hsa-miR-130b-3p predicted target genes. A. hsa-miR-193b-3p prodected target genes. B. hsa-miR-505-3p prodected target genes. C. hsa-miR-200a-3p predicted target genes. D. hsa-miR-194-5p predicted target genes. E. hsa-miR-130b-3p predicted target genes. The red and quadrate note represents the miRNAs. The blue-black circle note represents the miRNAs regulated target genes. The node size reflects it's correlation with the Edges.
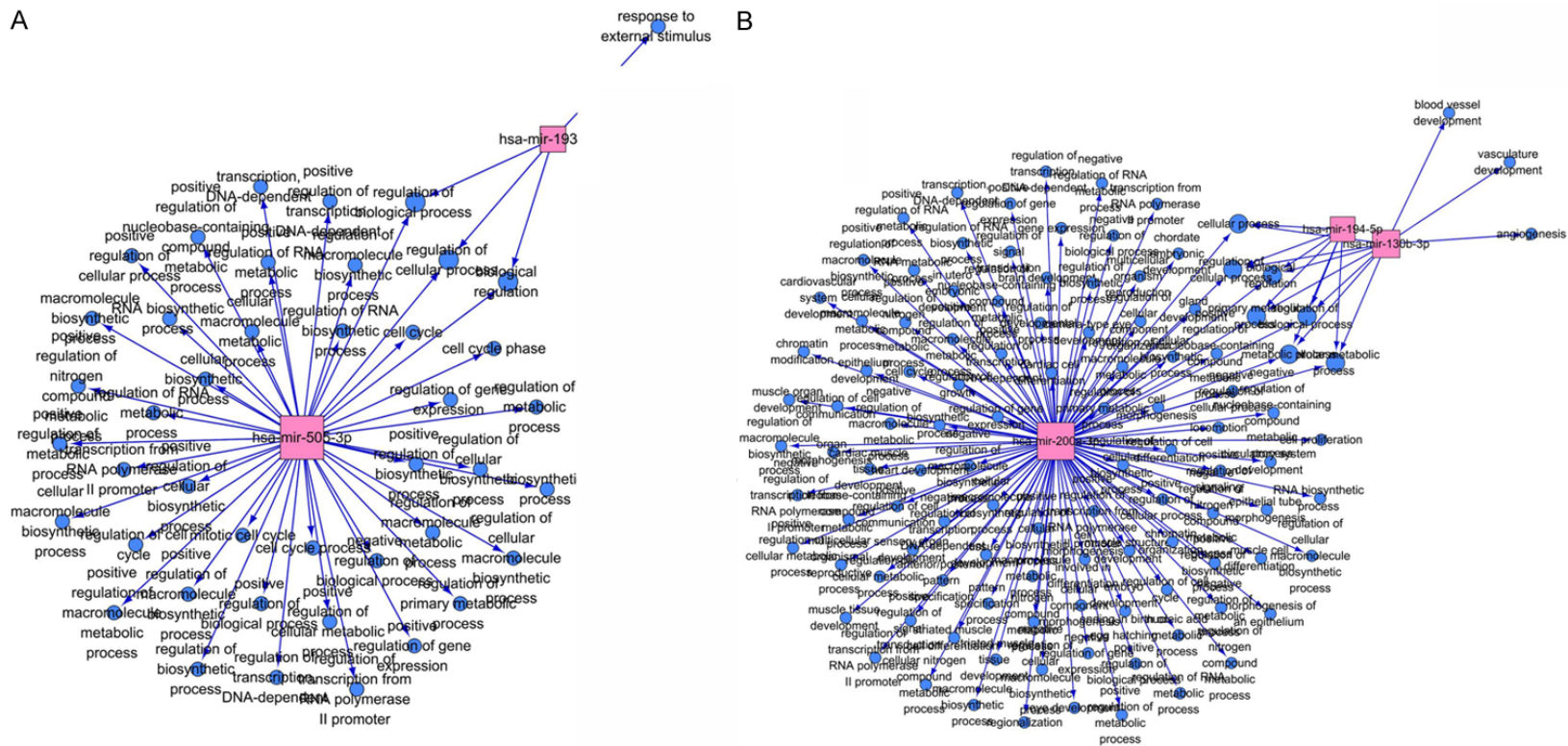
Figure 8. GO network for the miRNAs. A. GO network for the hsa-miR-193b-3p and hsa-miR-505-3p. B. GO network for the hsa-miR-200a-3p, hsa-miR-194-5p and hsa-miR-130b-3p. The red and quadrate note represents the miRNAs. The blue-black circle note represents the function terms. The node size reflects it's correlation with the Edges.

Go analysis

The GO analysis results showed that the up-expressed hsa-miR-193b-3p was correlated with 4 GO terms, and up-expressed hsa-miR-505-3p was correlated with 42 GO terms (**Figure 8A**; Supplementary Table 2). The down-expressed hsa-miR-200a-3p was correlated with 10 GO terms, hsa-miR-194-5p was correlated 7 GO terms and hsa-miR-130b-3p was correlated with 109 GO terms (**Figure 8B**; Supplementary Table 3).

Discussion

Isolation and identification of CSC is the basis for the study of cancer nature. Currently, the study on the CSC is still in the exploratory stage. Due to lack of the surface markers, the specific identification and sorting methods have not been established in majority of tumors. There are mainly two methods for sorting the cancer stem cells, including fluorescence activated cell sorting (FACS) and magnetic activated cell sorting (MACS) method (by using the Hoechst33342 dye). Since majority of the cancer stem cells lack the specific markers, the SP cell sorting is an ideal research approach to study the specific markers for cancer stem cells.

Goodell et al. [13] found that there is a very small part of the cells can discharg the intra-nuclear Hoechst33342 dye to the outside of cells, which were called the SP cells. Subsequently, the other researchers [14-19] isolated the stem cells featured SP cells in a variety of normal tissues. Kondo et al. [20] firstly isolated the SP cells from the C6 glioma cell lines, and which accounts for 0.4% of the total glioma cells. They also confirmed that the SP C6 glioma cells can form tumors in nude mice after transplantation in a variety of tissues, and can differentiate into neuron and neurogliocyte. These results indicate that the SP cells possess the characteristics of multiple differentiation potential as the tumor stem cells. In the following years, the SP cells were also isolated from a series of other malignancies and tumor cell lines, such as thyroid cancer [21], ovarian cancer [22], neuroblastoma [23], breast cancer [24], bone sarcomas [25], gastrointestinal cancers [26], bladder cancer [27], esophageal carcinoma [28], nasopharyngeal carcinoma [29], lung cancer [30], renal epithe-lial carcinoma [31], endometrial carcinoma [32], malignant mesothelioma [33] and pancreatic cancer [34] and ect. Similarly, all of the isolated SP cells characterize with the feature of tumor stem cells.

The previous study shows that the efflux characteristics (Hoechst33342) of SP cells were caused by the multidrug resistance gene, ABCG2 [18]. ABCG2 is a kind of transmembrane protein, which could efflux the fluorescent dye Hoechst 33342 to the outside of cells. Therefore, this population of cells showed fluorescence negative or low fluorescence intensity, which was named SP cells. Zhou et al. [18] found that when the ABCG2 gene was knock-outed from the bone marrow cells the SP phenotype almost completely lost, thus the ABCG2 in bone marrow cells is the critical factor that determines the SP phenotype. Therefore, the SP cells act as one of the surface marker of the stem cells, and could be used for isolating the stem cells with unknown surface markers.

In the isolation process of stem cells, the previous researchers attempted to identify the hepatocellular carcinoma stem cells by using the surface markers, such as CD133, CD90 and other markers [11, 12]. Chiba et al. [35] successfully separated 0.25% SP cells and 0.8% NSP cells from huh7 PLC/PRF/5 hepatoma cell lines. And proved the SP cells with higher proliferative and antiapoptotic capacity, and stronger tumorigenicity compared to NSP cells. Subsequently, some scientists also isolated the cancer stem cells featured SP cells in many different hepatocellular carcinoma cell lines [36-40]. The above results suggest that the stem cell featured SP cells really exist in the hepatocellular carcinoma cell lines. The current research on the hepatocellular carcinoma mainly focus on the hepatocellular carcinoma cell lines, however, whether the SP cells exist in th hepatocellular carcinoma tissues is also elusive [35-41]. This study sorted the SP cells and NSP cells from 10 cases of hepatocellular carcinoma tissues by using the flow cytometry fluorescence-activated cell sorting technique, and the results showed that percentage of SP cells range from 0.4% to 0.9% in hepatocellular carcinoma tissues. Meanwhile, when adding the calcium channel blocker, verapamil, the SP percentage was reduced to the levels of 0.00% to 0.02%. In this study, we used the RT-PCR

assay to detect the mRNA expression of SP and NSP cells, and found that SP cells expressed higher ABCG2, and NSP cells do not express ABCG2.

Cancer stem cells can not be easily cleared easily, and lead the metastasis and recurrence of the cancer. Benchaouir et al. [42] found that majority of the SP cells are the quiescent cells at the phase of G0. The present cell cycle analysis results showed that the hepatocellular carcinoma SP cells are mainly the quiescent cells retaining in the G0 phase, and NSP cells in the multi-plication phase. This result suggests that hepatocellular carcinoma SP cells possess the relatively quiescent characteristics of the cancer stem cells, which is consistent with the Zhang et al.'s report [39]. Anti-apoptosis function is another characteristic of the cancer stem cells, and the majority of tumor cells develop to the apoptotic cells post the limited proliferation and updated, and minority of tumor cells become the "seed" for tumor growth [43]. Chiba et al. [35] isolated the SP cells with strong anti-apoptotic function in both of Huh7 and PLC/PRF/5 cell lines. In this study, the apoptosis results indicated that the apoptosis rate in NSP cells was significantly higher compared to the SP cells in hepatocellular carcinoma SP cells. Therefore, the above results suggest that hepatocellular carcinoma SP cells have significant anti-apoptotic properties.

Strong self-proliferation, self-renewal capacity and pluripotency are the main characteristics of the cancer stem cells [20-34]. In this study, the cell proliferation results showed that the SP cells have the stronger proliferative ability compared to the NSP cells. The colony formation experiments showed that the colony formation rate in SP cells was higher significantly compared to the NSP cells, and the SP cells with high-density and length diameter of colony. These results suggest that hepatocellular carcinoma tissues derived SP cells with stronger cell proliferation, clonogenic capacity and multipotent differentiation capacity compared to the NSP cells, which is consistent with the characteristics of cancer stem cells.

Invasion and metastasis are the most important biological characteristics for malignant tumors. The cancer stem cell theory holds that the migration of cancer stem cells play important role in the tumor invasion and tumor metastasis [44]. The cell invasion results proved that there were more invasive cells passing artificial basement membrane in SP cell group compared to the NSP cell group after 48 h treatment. This result suggests that the invasive capability of SP cells was higher significantly compared to NSP cells, and there may be the cancer stem cell subpopulations in the SP cells. Also, the SP existence may be one of the reasons for tumor metastasis and recurrences of hepatocellular carcinoma. Migration and metastasis of tumor cells always be regulated by specific chemokines and their receptors [45]. Karnoub et al. [46] found that chemokines CCL5 and its receptor CCR5 can promote cancer invasion and transfer capability. All of above resutls and documents suggest that SP could trigger the chemokines, digestive enzyme production, and lead to tumor cell invasion and metastasis.

Compared with the non-cancer stem cells, highly tumorigenic is one of the most notable feature of the cancer stem cells [47]. So far, tumor xenograft experiments in vivo is also the gold standard for identifying the cancer stem cells. Since the mechanism for the stronger tumorigenicity of SP cells is also not fully clear, the tumor formation rate in SP cell transplantated immunodeficient mice was dessigned as a dominant criteria for evaluating the properties of cancer stem cells [48]. We transplated the selected SP cells into the nude mice, and observed their tumorigenicity. The results showed that the number of SP cells can form a clear xenografts at 1×10^3 concentration, and NSP cells at least 1×10^5 concentration. Our results also indicated that the tumor size in SP cell transplanted mice was larger significantly compared to NSP cells when treated with same concentration of SP cells, and also with a shorter latency for tumor formation. These results suggest that SP cells characterize with significantly higher tumorigenic capacity compared to NSP cells, which is consistent with the reports of Chiba et al. [35, 38]. The above findings may associate with the enrichment of cancer stem cels in SP SP cell subpopulation. The constantly self-renewing and asymmetric division continued proliferation of cancer stem cells in nude mice lead to the formation of nascent tumor.

microRNA is a class of endogenous small fragments of non-coding single-stranded RNA molecules that play a very important role in the

regulation of gene expression [49]. Many microRNAs play the role of oncogenes and tumor suppressor genes, which could also regulate the tumor cell differentiation and apoptosis processes [50]. The cancer stem cell associated microRNA study discovered that miRNA regulates self-renewal and differentiation of tumor stem cells through multiple regulation of target genes [51]. Based on the results of current research on hepatocellular carcinoma SP cells, we hypothesized that there may be some specific miRNA in regulating the activity of cancer stem cells, which play an important role in the life of hepatocellular carcinoma SP cells. Therefore, we used the high-throughput microarray technology to detect the miRNA expression profles of SP cells and NSP cells isolated from HCC tissues, and screen the differentialy expressed microRANs. According to the microarray results, we found that there were significant differences for the miRNA expressing profile between hepatocellular carcinoma SP cells and NSP cells. There were 107 miRNAs with the differential expression over 2-folds, including 45 up-regulated miRNAs and 62 down-regulated miRNAs. We could found that, in the SP cells, the down-regulated miRNAs are significantly more compared to the up-regulated miRNAs. This result suggest that the SP cells regulating the hepatocellular carcinoma progresses and development mainly by down-regulating some related miRNAs.

In conclusion, the results showed that the SP cells isolated from human hepatocellular carcinoma by using FACS sorting method plays critical role in the cell proliferation, colony formation, anti-apoptosis, self-renewal capacity, invasiveness, tumorigenicity and enhancement of ABCG2 gene expression, all of which levels were also higher compared to NSP cells. These findings suggest that sorted SP cells possess the cancer stem cells associated biological characteristics, meanwhile, also prove that it is feasible to sort and enrich the hepatocellular carcinoma stem cells by using the SP cells phenotype. Furthermore, screening the miRNAs by microarray study could discover the differentially expressed miRNAs between SP cells and NSP cells, which could provid a foundation for further investigating the functions of the hepatocellular carcinoma stem cells.

Address correspondence to: Dr. Qing Mao, Department of Infectious Diseases, Southwest Hospital, Third Military Medical University, No. 30 Gaotanyan Street, Chongqing 400038, China. Tel: +86-023-68754479; Fax: +86-023-68754475; E-mail: qingmaocq@sina.com

References

[1] Lilovet JM, Burroughs A, Bruix J. Hepatocellular carcinoma. Lancet 2003; 362: 1907-1917.

[2] Xu H, Mu J, Xiao J, Wu X, Li M, Liu T, Liu X. CD24 negative lung cancer cells, possessing partial cancer stem cell properties, cannot be considered as cancer stem cells. Am J Cancer Res 2015; 6: 51-60.

[3] Sottoriva A, Verhoeff JJ, Borovski T, McWeeney SK, Naumov L, Medema JP, Sloot PM, Vermeulen L. Cancer stem cell tumor model reveals invasive morphology and increased phenotypical heterogeneity. Cancer Res 2010; 70: 46-56

[4] Shervington A, Lu C. Expression of multidrug resistance genes in normal and cancer stem cells. Cancer Invest 2008; 26: 535-542.

[5] Bonnet D, Dick JE. Human acute myeloid leukemia is organized as a hierarchy that originates from a primitive hematopoietic cell. Nat Med 1997; 3: 730-737.

[6] Al-Hajj M, Wicha MS, Benito-Hernandez A. Prospective identification of tumorigenic breast cancer cells. Proc Natl Acad Sci U S A 2003; 100: 3983-3988.

[7] Patrawala L, Calhoun T, Schneider-Broussard R, Li H, Bhatia B, Tang S, Reilly JG, Chandra D, Zhou J, Claypool K, Coghlan L, Tang DG. Highly purified CD44+ prostate cancer cells from xenograft human tumors are enriched in tumorigenic and metastatic progenitor cells. Oncogene 2006; 25: 1696-1708.

[8] O'brien CA, Pollett A, Gallinger S, Dick JE. A human colon cancer cell capable of initiating tumor growth in immunodeficient mice. Nature 2007; 445: 106-110.

[9] Li C, Heidt DG, Dalerba P. Identification of pancreatic cancer stem cells. Cancer Res 2007; 67: 1030-1037.

[10] Lee JS, Gil JE, Kim JH, Kim TK, Jin X, Oh SY, Sohn YW, Jeon HM, Park HJ, Shin YJ, Chung TG, Lee JB, You S, Kim H. Brain cancer stem-like cell genesis from p53-deficient mouse astrocytes by oncogenic Ras. Biochem Biophys Res Commun 2008; 365: 496-502.

[11] Ma S, Chan KW, Hu L, Lee TK, Wo JY, Ng IO, Zheng BJ, Guan XY. Identification and characterization of tumorigenic liver cancer stem/progenitor cells. Gastroenterology 2007; 132: 2542-2556.

[12] Yamashita T, Ji J, Budhu A, Forgues M, Yang W, Wang HY, Jia H, Ye Q, Qin LX, Wauthier E, Reid LM, Minato H, Honda M, Kaneko S, Tang ZY, Wang XW. EpCAM-positive hepatocellular carcinoma cells are tumor-initiating cells with stem/progenitor cell features. Gastroenterology 2009; 136: 1012-1024.

[13] Goodell MA, Brose K, Paradis G, Conner AS, Mulligan RC. Isolation and functional properties of murine hematopoietic stem cells that are replicating in vivo. J Exp Med 1996; 183: 1797-1806.

[14] Inowa T, Hishikawa K, Takeuchi T, Kitamura T, Fujita T. Isolation and potential existence of side population cells in adult human kidney. Int J Urol 2008; 15: 272-274.

[15] Kobayashi M, Yakuwa T, Sasaki K, Sato K, Kikuchi A, Kamo I, Yokoyama Y, Sakuragawa N. Multilineage potential of side population cells from human amnion mesenchymal layer. Cell Transplant 2008; 17: 291-301.

[16] Martin J, Helm K, Ruegg P, Varella-Garcia M, Burnham E, Majka S. Adult lung side population cells have mesenchymal stem cell potential. Cytotherapy 2008; 10: 140-151.

[17] Hussain SZ, Strom SC, Kirby MR, Burns S, Langemeijer S, Ueda T, Hsieh M, Tisdale JF. Side population cells derived from adult human liver generate hepatocyte-like cells in vitro. Dig Dis Sci 2005; 50: 1755-1763.

[18] Zhou S, Schuetz JD, Bunting KD, Colapietro AM, Sampath J, Morris JJ, Lagutina I, Grosveld GC, Osawa M, Nakauchi H, Sorrentino BP. The ABC transporter Bcrp1/ABCG2 is expressed in a wide variety of stem cells and is a molecular determinant of the side population phenotype. Nat Med 2001; 7: 1028-1034.

[19] Falciatori I, Borsellino G, Haliassos N, Boitani C, Corallini S, Battistini L, Bernardi G, Stefanini M, Vicini E. Identification and enrichment of spermatogonial stem cells displaying side-2population phenotype in immature mouse testis. FASEB J 2004; 18: 376-388.

[20] Kondo T, Setoguchi T, Taga T. Persistence of a small subpopulation of cancer stem-like cells in the C6 glioma cell line. Proc Natl Acad Sci U S A 2004; 101: 781-786.

[21] Mitsutake N, Iwao A, Nagai K, Namba H, Ohtsuru A, Saenko V, Yamashita S. Characterization of side population in thyroid cancer cell lines: cancer stem-like cells are enriched partly but not exclusively. Endocrinology 2007; 48: 1797-1803.

[22] Zhang S, Balch C, Chan MW, Lai HC, Matei D, Schilder JM, Yan PS, Huang TH, Nephew KP. Identification and characterization of ovarian cancer initiating cells from p rimary human tumors. Cancer Res 2008; 68: 4311-4320.

[23] Qi S, Zheng J, Zhu H, Yang L, Xiao X. Identification of neuroblastoma stem cells by characterization of side population cells in the human neuroblastoma SK-N-SH cell line. J Pediatr Surg 2010; 45: 2305-2311.

[24] Christgen M, Ballmaier M, Bruchhardt H, von Wasielewski R, Kreipe H, Lehmann U. Identification of a distinct side population of cancer cells in the Cal- 51 human breast carcinoma cell line. Mol Cell Biochem 2007; 306: 201-212.

[25] Murase M, Kano M, Tsukahara T, Takahashi A, Torigoe T, Kawaguchi S, Kimura S, Wada T, Uchihashi Y, Kondo T, Yamashita T, Sato N. Side population cells have the characteristics of cancer stemlike cells/cancer-initiating cells in bone sarcomas. Br J Cancer 2009; 101: 1425-1432.

[26] Haraguchi N, Inoue H, Tanaka F, Mimori K, Utsunomiya T, Sasaki A, Mori M. Cancer stem cells in human gastrointestinal cancers. Hum Cell 2006; 19: 24-29.

[27] She JJ, Zhang PG, Wang ZM, Gan WM, Che XM. Identification of side population cells from bladder cancer cells by DyeCycle Violet staining. Cancer Biol Ther 2008; 7: 1663-1668.

[28] Huang D, Gao Q, Guo L, Zhang C, Jiang W, Li H, Wang J, Han X, Shi Y, Lu SH. Isolation and identification of cancer stem-like cells in esophageal carcinoma cell lines. Stem Cells Dev 2009; 18: 465-473.

[29] Wang J, Guo LP, Chen LZ, Zeng YX, Lu SH. Identification of cancer stem cell-like side population cells in human nasopharyngeal carcinoma cell line. Cancer Res 2007; 67: 3716-3724.

[30] Ho MM, Ng AV, Lam S, Hung JY. Side population in human lung cancer cell lines and tumors is enriched with stem2like cancer cells. Cancer Res 2007; 67: 4827-4833.

[31] Addla SK, Brownl MD, Hart CA, Ramani VA, Clarke NW. Characterization of the Hoechsd-3342 side population from normal and malignant human renal epithelial cells. Am J Physiol Renal Physiol 2008; 295: 680-687.

[32] Friel AM, Sergent PA, Patnaude C, Szotek PP, Oliva E, Scadden DT, Seiden MV, Foster R, Rueda BR. Functional analyses of the cancer

stem cell-like properties of human endometrial tumor initiating cells. Cell Cycle 2008; 7: 242-249.

[33] Kai K, D'Costa S, Yoon BI, Brody AR, Sills RC, Kim Y. Characterization of side population cells in human malignant mesothelioma cell lines. Lung Cancer 2010; 70: 146-151.

[34] Yao J, Cai HH, Wei JS, An Y, Ji ZL, Lu ZP, Wu JL, Chen P, Jiang KR, Dai CC, Qian ZY, Xu ZK, Miao Y. Side population in the pancreatic cancer cell lines SW1990 and CFPAC-1 is enriched with cancer stem-li ke cells. Oncol Rep 2010; 23: 1375-1382.

[35] Chiba T, Kita K, Zheng YW, Yokosuka O, Saisho H, Iwama A, Nakauchi H, Taniguchi H. Side population purified from hepatocellular carcinoma cells harbors cancer stem cell-like properties. Hepatology 2006; 44: 240-251.

[36] Haraguchi N, Utsunomiya T, Inoue H, Tanaka F, Mimori K, Barnard GF, Mori M. Characterization of a side population of cancer cells from human gastrointestinal system. Stem Cells 2006; 24: 506-513.

[37] Fan J, Li R, Zhang R, Liu HL, Zhang N, Zhang FQ, Dou KF. Effect of Bcl-2 and Bax on survival of side population cells from hepatocellular carcinoma cells. World J Gastroenterol 2007; 13: 6053-6059.

[38] Shi GM, Xu Y, Fan J, Zhou J, Yang XR, Qiu SJ, Liao Y, Wu WZ, Ji Y, Ke AW, Ding ZB, He YZ, Wu B, Yang GH, Qin WZ, Zhang W, Zhu J, Min ZH, Wu ZQ. Identification of side population cells in human hepatocellular carcinoma cell lines with stepwise metastatic potentials. J Cancer Res Clin Oncol 2008; 134: 1155-1163.

[39] Zhang N, Li R, Tao KS, Cao DY, Ti ZY, Ding R, Cai L, Zhang FQ, Dou KF. Characterization of a stem-like population in hepatocellular carcinoma MHCC97 cells. Oncol Rep 2010; 23: 827-831.

[40] Zhang Y, Song WJ, Zhang FQ, Liu WH, Dou KF. Differentiation-inducing activity of hydroxycamptothecin on cancer stem-like cells derived from hepatocellular carcinoma. Dig Dis Sci 2011; 56: 2473-2481.

[41] Song Z, Li R, You N, Tao K, Dou K. Loss of heterozygosity of the tumor suppressor gene Tg737 in the side population cells of hepatocellular carcinomas is associated with poor prognosis. Mol Biol Rep 2010; 37: 4091-4101

[42] Benchaouir R, Rameau P, Decraene C, Dreyfus P, Israeli D, Pietu G, Danos O, Garcia L. Evidence for a resident subset of cells with SP phenotype in the C2C12 myogenic line: a tool to explore muscle stem cell biology. Exp Cell Res 2004; 294: 254-268.

[43] Chen W, Wang G, Lin Y. Apoptosis resistance can be used in screening the markers of cancer stem cells. Med Hypotheses 2006; 67: 1381-1383.

[44] Vasko V, Espinosa AV, Scouten W, He H, Auer H, Liyanarachchi S, Larin A, Savchenko V, Francis GL, de la Chapelle A, Saji M, Ringel MD. Gene expression and functional evidence of epithelial-to-mesenchymal transition in papillary thyroid carcinoma invasion. Proc Natl Acad Sci U S A 2007; 104: 2803-2808.

[45] Tu SM, Lin SH, Logothetis CJ. Stem2 cell origin of metastasis and heterogeneity in solid tumours. Lancet Oncol 2002; 3: 508-513.

[46] Karnoub AE, Dash AB, Vo AP, Sullivan A, Brooks MW, Bell GW, Richardson AL, Polyak K, Tubo R, Weinberg RA. Mesenchymal stem cells within tumour stroma promote breast cancer metastasis. Nature 2007; 449: 557-563.

[47] Eramo A, Lotti F, Sette G, Pilozzi E, Biffoni M, Di Virgilio A, Conticello C, Ruco L, Peschle C, De Maria R. Identification and expansion of the tumorigenic lung cancer stem cell population. Cell Death Differ 2008; 15: 504-514.

[48] Asakura A, Rudnicki MA. Side population cells from diverse adult tissues are capable of in vitro hematopoietic differentiation. Exp Hematol 2002; 30: 1339-1345.

[49] Li Y, Chen P, Zu L, Liu B, Wang M, Zhou Q. Micro-RNA-338-3p suppresses metastasis of lung cancer cells by targeting the EMT regulator Sox4. Am J Cancer Res 2016; 6: 127-140.

[50] He Y, Wang J, Wang J, Yung VY, Hsu E, Li A, Kang Q, Ma J, Han Q, Jin P, Xing P, Lu Y, Sheng J. Micro-RNA-135b regulates apoptosis and chemoresistance in colorectal cancer by targeting large tumor suppressor kinase 2. Am J Cancer Res 2015; 5: 1382-1395.

[51] Jones MF, Hara T, Francis P, Li XL, Bilke S, Zhu Y, Pineda M, Subramanian M, Bodmer WF, Lal A. The CDX1-microRNA-215 axis regulates colorectal cancer stem cell differentiation. Proc Natl Acad Sci U S A 2015; 112: e1550-1558.

Supplementary Table 1. Relative miRNA over and under expression levers in SP cells compared to NSP cells

Overexpression miRNA	Fold chang	Underexpression miRNA	Fold chang
hsa-miR-193b-3p	13.57466084	hsa-miR-200a-3p	0.07719342
hsa-miR-16-2-3p	11.47780862	hsa-miR-4300	0.145005846
hsa-miR-4534	9.08514122	hsa-miR-192-5p	0.159719808
hsa-miR-100-5p	7.143027698	hsa-miR-194-5p	0.160584747
hsa-miR-10b-5p	6.310873043	hsa-miR-4278	0.163524047
hsa-miR-505-3p	6.192544174	hsa-miR-130b-3p	0.18297662
hsa-miR-378g	5.233099862	hsa-miR-625-5p	0.199282377
hsa-miR-452-5p	5.212948414	hsa-miR-519d-3p	0.227617082
hsa-miR-30c-1-3p	4.630349752	hsa-miR-125a-3p	0.227880183
hsa-miR-711	4.164632636	hsa-miR-548an	0.24151949
hsa-miR-4484	3.854213293	hsa-miR-320e	0.256139137
hsa-miR-3660	3.821604119	hsa-miR-671-5p	0.266510167
hsa-miR-4691-3p	3.577487707	hsa-miR-410-5p	0.268751841
hsa-miR-4441	3.47725102	hsa-miR-29a-5p	0.270733183
hsa-miR-29c-3p	3.472237777	hsa-miR-935	0.281542426
hsa-miR-3687	3.297569776	hsa-miR-377-5p	0.284469442
hsa-miR-3678-3p	3.24535561	hsa-miR-3168	0.287489676
hsa-miR-614	3.103428902	hsa-miR-193a-5p	0.295295852
hsa-miR-190a-5p	3.10118546	hsa-miR-320d	0.29643431
hsa-miR-188-3p	3.042233819	hsa-miR-29a-3p	0.29825148
hsa-miR-505-5p	3.034803271	hsa-miR-323a-3p	0.30054815
hsa-miR-1205	2.946057806	hsa-miR-3650	0.301641052
hsa-miR-3193	2.850559773	hsa-miR-548j-5p	0.304154728
hsa-miR-4451	2.784405236	hsa-miR-514a-5p	0.312182272
hsa-miR-3924	2.666901022	hsa-miR-4429	0.315398292
hsa-miR-365a-3p/hsa-miR-365b-3p	2.622838246	hsa-miR-3132	0.316941685
hsa-miR-17-3p	2.585948569	hsa-let-7c-5p	0.3281603
hsa-miR-638	2.545096379	hsa-miR-135a-5p	0.329441873
hsa-miR-5187-3p	2.491511846	hsa-miR-320c	0.33470381
hsa-miR-708-5p	2.437994886	hsa-miR-1293	0.345997869
hsa-miR-874-3p	2.424988459	hsa-miR-222-3p	0.351750135
hsa-miR-196a-5p	2.406334701	hsa-miR-4689	0.352831005
hsa-miR-23a-5p	2.348092054	hsa-miR-4436b-5p	0.353509808
hsa-miR-30a-5p	2.322331995	hsa-miR-25-5p	0.359129106
hsa-miR-365b-5p	2.313209138	hsa-miR-130b-5p	0.363086452
hsa-miR-378f	2.311149827	hsa-miR-7-5p	0.365069496
hsa-miR-3607-3p	2.287527279	hsa-miR-4443	0.369798051
hsa-miR-186-5p	2.231394649	hsa-miR-323b-5p	0.371031978
hsa-miR-663b	2.158673905	hsa-miR-29b-3p	0.378771673
hsa-miR-30e-5p	2.130916411	hsa-miR-361-5p	0.379681757
hsa-miR-33a-5p	2.077003916	hsa-miR-4677-3p	0.39316462
hsa-miR-2355-3p	2.051687143	hsa-miR-320b	0.395999646
hsa-miR-618	2.027698185	hsa-miR-4657	0.407521803
hsa-miR-101-3p	2.020048392	hsa-miR-125b-1-3p	0.408866005
hsa-miR-16-1-3p	2.011918433	hsa-miR-216a-3p	0.435433998

hsa-miR-4717-3p	0.436585734
hsa-miR-605-5p	0.44621064
hsa-miR-335-3p	0.446730373
hsa-miR-664b-3p	0.44887334
hsa-miR-612	0.456962456
hsa-miR-4711-3p	0.457274724
hsa-miR-431-3p	0.461691279
hsa-miR-3175	0.46633083
hsa-miR-9-5p	0.470308882
hsa-miR-4714-5p	0.471558215
hsa-miR-4483	0.478016318
hsa-miR-5681b	0.482739428
hsa-miR-221-3p	0.490147788
hsa-miR-942-5p	0.498031133
hsa-miR-642b-5p	0.498041789
hsa-miR-126-3p	0.498757753
hsa-miR-4709-3p	0.498840837

Supplementary Table 2. GO analysis for hsa-miR-193b-3p and hsa-miR-505-3p

miRNAs	GO terms
hsa-mir-193b-3p	Response to external stimulus
	Regulation of biological process
	Regulation of cellular process
	Biological regulation
hsa-mir-505-3p	Mitotic cell cycle
	Transcription, DNA-dependent
	Regulation of transcription, DNA-dependent
	Regulation of transcription from RNA polymerase II promoter
	Transcription from RNA polymerase II promoter
	Cell cycle
	Biosynthetic process
	Macromolecule biosynthetic process
	Regulation of biosynthetic process
	Positive regulation of biosynthetic process
	Positive regulation of metabolic process
	Regulation of gene expression
	Regulation of macromolecule biosynthetic process
	Positive regulation of macromolecule biosynthetic process
	Positive regulation of macromolecule metabolic process
	Positive regulation of gene expression
	Regulation of metabolic process
	Cell cycle process
	Cell cycle phase
	Positive regulation of cellular metabolic process
	Regulation of cellular biosynthetic process
	Positive regulation of cellular biosynthetic process
	RNA biosynthetic process
	Cellular macromolecule biosynthetic process
	Cellular biosynthetic process
	Cellular macromolecule metabolic process
	Positive regulation of transcription, DNA-dependent
	Positive regulation of nucleobase-containing compound metabolic process
	Positive regulation of biological process
	Negative regulation of biological process
	Positive regulation of cellular process
	Regulation of biological process
	Regulation of cellular process
	Positive regulation of nitrogen compound metabolic process
	Regulation of RNA metabolic process
	Positive regulation of RNA metabolic process
	Regulation of cell cycle
	Regulation of macromolecule metabolic process
	Biological regulation
	Regulation of primary metabolic process
	Regulation of cellular macromolecule biosynthetic process
	Regulation of RNA biosynthetic process

Supplementary Table 3. Go analysis for hsa-miR-200a-3p, hsa-miR-194-5p andhsa-miR-130b-3p

miRNAs	GO terms
hsa-mir-130b-3p	Angiogenesis
	Blood vessel development
	Vasculature development
	Metabolic process
	Cellular process
	Cellular metabolic process
	Primary metabolic process
	Regulation of biological process
	Regulation of cellular process
	Biological regulation
hsa-mir-194-5p	Metabolic process
	Cellular process
	Cellular metabolic process
	Primary metabolic process
	Regulation of biological process
	Regulation of cellular process
	Biological regulation
hsa-mir-200a-3p	Negative regulation of transcription from RNA polymerase II promoter
	Cell morphogenesis
	Cell morphogenesis involved in differentiation
	Eye development
	In utero embryonic development
	Morphogenesis of an epithelium
	Regionalization
	Nucleobase-containing compound metabolic process
	Chromatin organization
	Transcription, DNA-dependent
	Regulation of transcription, DNA-dependent
	Regulation of transcription from RNA polymerase II promoter
	Transcription from RNA polymerase II promoter
	Nitrogen compound metabolic process
	Cell cycle
	Pattern specification process
	Brain development
	Sensory organ development
	Heart development
	Muscle organ development
	Metabolic process
	Cell proliferation
	Biosynthetic process
	Macromolecule biosynthetic process
	Embryo development ending in birth or egg hatching
	Organ morphogenesis
	Tissue development
	Regulation of biosynthetic process
	Positive regulation of biosynthetic process
	Negative regulation of metabolic process

Positive regulation of metabolic process

Anterior/posterior pattern specification

Regulation of signal transduction

Positive regulation of signal transduction

Cellular process

Gene expression

Regulation of gene expression

Regulation of macromolecule biosynthetic process

Positive regulation of macromolecule biosynthetic process

Negative regulation of macromolecule biosynthetic process

Positive regulation of macromolecule metabolic process

Negative regulation of macromolecule metabolic process

Positive regulation of gene expression

Negative regulation of gene expression

Regulation of cell communication

Positive regulation of cell communication

Striated muscle tissue development

RNA metabolic process

Chromatin modification

Regulation of nucleobase-containing compound metabolic process

Positive regulation of signaling

Regulation of cellular metabolic process

Positive regulation of cellular metabolic process

Regulation of cellular biosynthetic process

Positive regulation of cellular biosynthetic process

Multicellular organism reproduction

RNA biosynthetic process

Cellular component morphogenesis

Cellular nitrogen compound metabolic process

Cellular macromolecule biosynthetic process

Cardiac cell differentiation

Regulation of growth

Locomotion

Muscle cell differentiation

Chordate embryonic development

Camera-type eye development

Macromolecule metabolic process

Cellular metabolic process

Primary metabolic process

Cellular biosynthetic process

Cellular macromolecule metabolic process

Regulation of cell differentiation

Negative regulation of transcription, DNA-dependent

Positive regulation of transcription, DNA-dependent

Negative regulation of nucleobase-containing compound metabolic process

Positive regulation of nucleobase-containing compound metabolic process

Positive regulation of transcription from RNA polymerase II promoter

Positive regulation of biological process

Negative regulation of biological process

Positive regulation of cellular process

Negative regulation of cellular process

Multicellular organismal reproductive process

Gland development

Cardiac muscle tissue development

Regulation of biological process

Regulation of developmental process

Regulation of cellular process

Regulation of cellular component organization

Striated muscle cell differentiation

Regulation of nitrogen compound metabolic process

Negative regulation of nitrogen compound metabolic process

Positive regulation of nitrogen compound metabolic process

Regulation of RNA metabolic process

Negative regulation of RNA metabolic process

Positive regulation of RNA metabolic process

Regulation of cell cycle

Regulation of macromolecule metabolic process

Epithelium development

Muscle tissue development

Epithelial tube morphogenesis

Muscle structure development

Biological regulation

Cardiovascular system development

Circulatory system development

Regulation of primary metabolic process

Nucleic acid metabolic process

Regulation of cellular macromolecule biosynthetic process

Negative regulation of cellular macromolecule biosynthetic process

Regulation of RNA biosynthetic process